

Resonances $X(4140)$, $X(4160)$, and $P_{cs}(4459)$ in the decay of $\Lambda_b \rightarrow J/\psi\Lambda\phi$

Wen-Ying Liu,¹ Wei Hao,^{2,3} Guan-Ying Wang,⁴ Yan-Yan Wang,⁵ En Wang^{1,*} and De-Min Li^{1,†}

¹*School of Physics and Microelectronics, Zhengzhou University, Zhengzhou, Henan 450001, China*

²*CAS Key Laboratory of Theoretical Physics, Institute of Theoretical Physics, Chinese Academy of Sciences, Beijing 100190, China*

³*University of Chinese Academy of Sciences (UCAS), Beijing 100049, China*

⁴*School of Physics and Electronics, Henan University, Kaifeng 475004, China*

⁵*School of Materials Science and Engineering, Zhengzhou University of Aeronautics, Henan 450001, China*



(Received 7 December 2020; accepted 1 February 2021; published 24 February 2021)

We study the decay of $\Lambda_b \rightarrow J/\psi\Lambda\phi$ by taking into account the intermediate resonances $X(4140)$, $X(4160)$, and $P_{cs}(4459)$. In addition to the peak of the $X(4140)$, we also find a bump structure around 4160 MeV followed by a cusp structure around $D_s^*\bar{D}_s^*$ threshold in the $J/\psi\phi$ invariant mass distribution of the $\Lambda_b \rightarrow J/\psi\Lambda\phi$ process, which can be associated to the $D_s^*\bar{D}_s^*$ molecular state $X(4160)$. We also show that this reaction can also be used to confirm the existence of the hidden-charm pentaquark $P_{cs}(4459)$ with strangeness. We predict an enhancement structure close to the threshold in the $D_s^*\bar{D}_s^*$ invariant mass distribution of the $\Lambda_b \rightarrow D_s^*\bar{D}_s^*\Lambda$ process, which is the reflection of the $X(4160)$ and should not be misidentified with a new resonance. We strongly suggest experimentalists to further measure these processes, which can be useful to clarify the nature of $X(4140)$ and $X(4160)$ resonances, and to confirm the existence of the $P_{cs}(4459)$.

DOI: [10.1103/PhysRevD.103.034019](https://doi.org/10.1103/PhysRevD.103.034019)

I. INTRODUCTION

In the last decades, a lot of exotic multi-quark states were observed experimentally, which demonstrates that there exist more complex configurations than the conventional mesons and baryons predicted by the classical quark model [1–3]. Many of them are reported in the weak decays of the heavy hadrons, and the theoretical studies on the weak decays of the heavy hadrons have also increased our understanding of hadron-hadron interactions and the nature of many intermediate exotic states [4,5].

It should be stressed that the weak decays of the Λ_b have been proved to be a rich source of exotic spectroscopy, such as the new pentaquark states $P_c(4312)^+$, $P_c(4380)^+$, and $P_c(4350)^+$ observed by the LHCb Collaboration [6,7]. Very recently, the CMS Collaboration has reported the observation of the $\Lambda_b \rightarrow J/\psi\Lambda\phi$ decay using proton-proton collision data at the LHC, the ratio of the branching fraction $\mathcal{B}(\Lambda_b \rightarrow J/\psi\Lambda\phi)/\mathcal{B}(\Lambda_b \rightarrow \psi(2s)\phi) = (8.26 \pm 0.90 \pm 0.68 \pm 0.11) \times 10^{-2}$ [8]. The observation of this reaction has

opened a window on future searches for new resonances in the $J/\psi\Lambda$ and $J/\psi\phi$ systems, once a sufficient number of signal events are accumulated, as mentioned by the CMS Collaboration [8].

A series of meson-baryon interactions in the hidden-charm sector, including the $J/\psi\Lambda$, were studied within the framework of the coupled channel unitary approach with the local hidden gauge formalism in Ref. [9], and two hidden charmonium pentaquark states were predicted in the isospin $I=0$ and strangeness $S=-1$ sector. Since the predicted hidden charm $S=-1$ pentaquark couples in S wave to $J/\psi\Lambda$ with a reasonable strength, some reactions involving the $J/\psi\Lambda$ final state system are proposed to search for the hidden charmonium pentaquark state, such as $\Lambda_b \rightarrow J/\psi K^0\Lambda$ [10], $\Xi_b \rightarrow J/\psi K^-\Lambda$ [11], $\Lambda_b \rightarrow J/\psi\eta\Lambda$ [12]. There are also some studies about the hidden-charm pentaquark state with strangeness [13–18]. Basing the suggestion proposed in Ref. [11], the LHCb has started to search for the hidden-charm pentaquark with strangeness in Ref. [19]. Very recently, the LHCb Collaboration reported a hidden-charm pentaquark state with strangeness $P_{cs}(4459)$ in the $J/\psi\Lambda$ invariant mass spectrum of the $\Xi_b^- \rightarrow J/\psi K^-\Lambda$ process, and the mass and width of $P_{cs}(4459)$ were measured to be [20]

$$\begin{aligned} M_{P_{cs}} &= 4458.8 \pm 2.9_{-1.1}^{+4.7} \text{ MeV}, \\ \Gamma_{P_{cs}} &= 17.3 \pm 6.5_{-5.7}^{+8.0} \text{ MeV}. \end{aligned} \quad (1)$$

*wangen@zzu.edu.cn

†lidm@zzu.edu.cn

Published by the American Physical Society under the terms of the [Creative Commons Attribution 4.0 International license](https://creativecommons.org/licenses/by/4.0/). Further distribution of this work must maintain attribution to the author(s) and the published article's title, journal citation, and DOI. Funded by SCOAP³.

Although the quantum numbers of the $P_{cs}(4459)$ have not been determined, a hidden-charm pentaquark with strangeness $S = -1$ and $J^P = 1/2^-$ was predicted to have a mass much close to the $P_{cs}(4459)$ mass in many works [15,16,21]. Thus, we will take into account the contribution from the $P_{cs}(4459)$ in the $J/\psi\Lambda$ system of the $\Lambda_b \rightarrow J/\psi\Lambda\phi$ process.

For the $J/\psi\phi$ system, one of the most important resonances is the charmoniumlike state $X(4140)$, which was first reported in the $B^+ \rightarrow J/\psi\phi K^+$ process by the CDF Collaboration [22] and later confirmed by the CMS [23], D0 [24,25], and LHCb Collaborations [26,27]. However, the width of the $X(4140)$ is measured to be $83 \pm 21_{-2.8}^{+4.6}$ MeV MeV by LHCb [26,27], much larger than the data from the other experiments [28], which confuses the understanding of the $X(4140)$ nature [29,30]. We have provided a reasonable explanation of the LHCb measurements [26,27] by considering the contributions from the $X(4160)$ and the $X(4140)$ with a narrow width, and have predicted a broad bump around 4160 MeV followed by a cusp at $D_s^*\bar{D}_s^*$ threshold in the $J/\psi\phi$ invariant mass distribution, which is one feature of the $D_s^*\bar{D}_s^*$ molecular state $X(4160)$ [31]. In addition, the predicted $J/\psi\phi$ invariant mass distribution of the $e^+e^- \rightarrow \gamma J/\psi\phi$ involving the intermediate $X(4140)$ and $X(4160)$ is also compatible with the BESIII measurement [32].

The S -wave interaction of ten vector-vector channels with charm $C = 0$ and strangeness $S = 0$ ($J/\psi\phi$, $D_s^*\bar{D}_s^*$, $D^*\bar{D}^*$, $K^*\bar{K}^*$, $\rho\rho$, $\omega\omega$, $\phi\phi$, $J/\psi J/\psi$, $\omega J/\psi$, $\omega\phi$) was studied within the hidden gauge formalism, and one $D^*\bar{D}^*$ molecular state with $I(J^{PC}) = 0(2^{++})$ was predicted, which could be identified as $X(4160)$ [33]. Based on the above discussions, we expect that the $X(4140)$ and $X(4160)$ play an important role in the reaction of $\Lambda_b \rightarrow J/\psi\Lambda\phi$.

In this work, we will study the reaction of $\Lambda_b \rightarrow J/\psi\Lambda\phi$ by taking into account the contributions from the $X(4140)$, $X(4160)$, and $P_{cs}(4459)$, and also propose to test the molecular nature of the $X(4160)$ by looking for the enhancement structure near the $D_s^*\bar{D}_s^*$ threshold in the $\Lambda_b \rightarrow D_s^*\bar{D}_s^*\Lambda$ reaction, since more data samples of those two processes are crucial to learn more about the charmoniumlike states $X(4140)$ and $X(4160)$ and especially to confirm the existence of the recently observed $P_{cs}(4459)$.

This paper is organized as follows. In Sec. II, we will present the mechanism for the reaction of $\Lambda_b \rightarrow J/\psi\Lambda\phi$ and $\Lambda_b \rightarrow D_s^*\bar{D}_s^*\Lambda$, and in Sec. III, we will show our results and discussions, followed by a short summary in the last section.

II. FORMALISM

A. The $\Lambda_b \rightarrow J/\psi\Lambda\phi$ process

Analogous to Refs. [8,10–12,31,34], the $\Lambda_b \rightarrow J/\psi\Lambda\phi$ process can perform through the W^- internal emission mechanism. In the first step, the b quark of the initial Λ_b

weakly decays into a c quark and a W^- boson, followed by the W^- decaying into $\bar{c}s$ pair, which can be expressed as

$$\begin{aligned} |\Lambda_b\rangle &= \frac{1}{\sqrt{2}}b(ud - du) \\ &\Rightarrow V_{bc} \frac{1}{\sqrt{2}}cW^-(ud - du) \\ &\Rightarrow V_{bc}V_{cs} \frac{1}{\sqrt{2}}c\bar{c}s(ud - du), \end{aligned} \quad (2)$$

where we take the flavor wave function $\Lambda_b = b(ud - du)/\sqrt{2}$, and V_{bc} and V_{cs} are the elements of the Cabibbo-Kobayashi-Maskawa (CKM) matrix. In order to give rise to the final states of this process, the quark components of Eq. (2), together with an extra $\bar{q}q$ ($\equiv \bar{u}u + \bar{d}d + \bar{s}s$) created from the vacuum, should hadronize into hadrons, as depicted in Fig. 1(a),

$$\begin{aligned} |H^{(a)}\rangle &= V_{bc}V_{cs}J/\psi \left| s(\bar{s}s) \frac{(ud - du)}{\sqrt{2}} \right\rangle \\ &= V_{bc}V_{cs}J/\psi\phi\Lambda. \end{aligned} \quad (3)$$

On the other hand, since the $X(4160)$ was predicted to strongly couple to the $D_s^*\bar{D}_s^*$ channel and weakly couple to the $J/\psi\phi$ channel [33], the $c\bar{c}sud$ component from the Λ_b weak decay, together with the extra $\bar{s}s$ created from the vacuum, could hadronize to the $D_s^*\bar{D}_s^*\Lambda$ in two ways: the W^- internal emission of Fig. 1(b) and the W^- external emission of Fig. 1(c). Although this is not the final state of $J/\psi\Lambda\phi$ that one observes, the idea is that $D_s^*\bar{D}_s^*$ will interact and create a resonance that couples to $J/\psi\phi$. We have

$$\begin{aligned} |H^{(b)}\rangle &= V_{bc}V_{cs} \left| c(\bar{s}s)\bar{c}s \frac{(ud - du)}{\sqrt{2}} \right\rangle \\ &= V_{bc}V_{cs}D_s^*\bar{D}_s^*\Lambda, \end{aligned} \quad (4)$$

$$\begin{aligned} |H^{(c)}\rangle &= V_{bc}V_{cs} \left| \bar{c}s c(\bar{s}s) \frac{(ud - du)}{\sqrt{2}} \right\rangle \\ &= V_{bc}V_{cs}\bar{D}_s^*D_s^*\Lambda, \end{aligned} \quad (5)$$

which finally produce $J/\psi\phi$ via the $D_s^*\bar{D}_s^*$ final state interaction.

Although we can straightly get the final state of $J/\psi\phi\Lambda$ via the mechanism of Fig. 1(a), this mechanism is penalized by a color factor with respect to the W^- external emission of Fig. 1(c), and this term with intermediate state $J/\psi\phi$ instead of $D_s^*\bar{D}_s^*$ would involve the extra factor $g_{J/\psi\phi}/g_{D_s^*\bar{D}_s^*} = |-2617 - i5151|/|18927 - i5524| \approx 0.3$ versus the amplitudes of Figs. 1(b) and 1(c), where $g_{J/\psi\phi} = (-2617 - i515)$ MeV and $g_{D_s^*\bar{D}_s^*} = (18927 - i5524)$ MeV are the couplings of the $D_s^*\bar{D}_s^*$ molecule to $J/\psi\phi$ and $D_s^*\bar{D}_s^*$ [33].

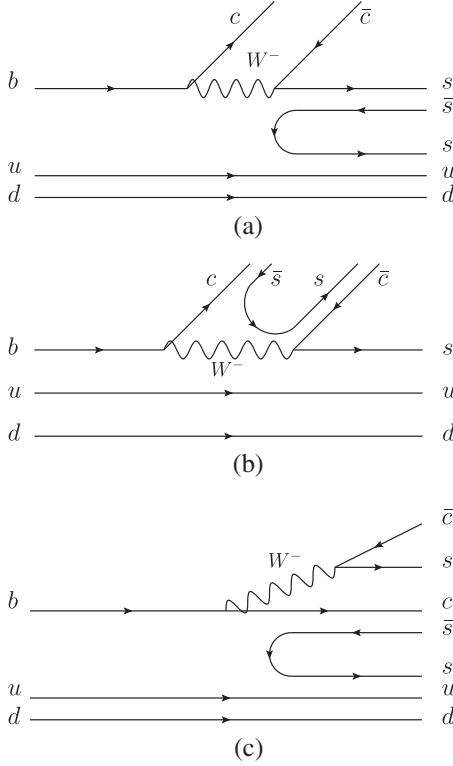


FIG. 1. The Λ_b weak decay at the microscopic quark picture. (a) The $\Lambda_b \rightarrow J/\psi \Lambda \phi$ decay through the internal W^- emission and hadronization of sud through $q\bar{q}$ created with vacuum quantum numbers. (b) The $\Lambda_b \rightarrow D_s^* \bar{D}_s^* \Lambda$ decay through the internal W^- emission and hadronization of $c\bar{c}$ through $s\bar{s}$. (c) The $\Lambda_b \rightarrow D_s^* \bar{D}_s^* \Lambda$ decay through the external W^- emission and hadronization of cud with $s\bar{s}$.

Thus, we will neglect the contribution from Fig. 1(a) in this work.

Now, we need the final state interaction of $D_s^* \bar{D}_s^*$ produced in Figs. 1(b) and 1(c) to give rise to the $J/\psi \phi$ final state and also generate dynamically the $D_s^* \bar{D}_s^*$ molecular state $X(4160)$, as shown in Fig. 2(a). Since the quantum numbers of $X(4160)$ are predicted to be $J^{PC} = 2^{++}$ in Refs. [33,35], Λ should be in P wave to match to the spin $J = 1/2$ of the initial Λ_b , and the amplitude can be expressed as

$$\mathcal{M}^P = A(\vec{\epsilon}_{J/\psi} \times \vec{\epsilon}_\phi) \cdot \vec{k} G_{D_s^* \bar{D}_s^*} t_{D_s^* \bar{D}_s^* \rightarrow J/\psi \phi}, \quad (6)$$

where the unknown constant A represents the total weight of the microscopic decay in the quark level showed in Figs. 1(b) and 1(c); $\vec{\epsilon}_{J/\psi}$ and $\vec{\epsilon}_\phi$ are the polarization vectors of the J/ψ and ϕ , respectively; \vec{k} is the Λ momentum in the rest frame of the $J/\psi \phi$ system; $G_{D_s^* \bar{D}_s^*}$ is the loop function of the $D_s^* \bar{D}_s^*$ channel, and $t_{D_s^* \bar{D}_s^* \rightarrow J/\psi \phi}$ is the transition amplitude of $D_s^* \bar{D}_s^* \rightarrow J/\psi \phi$, both of which are the functions of the $J/\psi \phi$ invariant mass $M_{J/\psi \phi}$. To avoid potential dangers using the dimensional regularizations as pointed out in

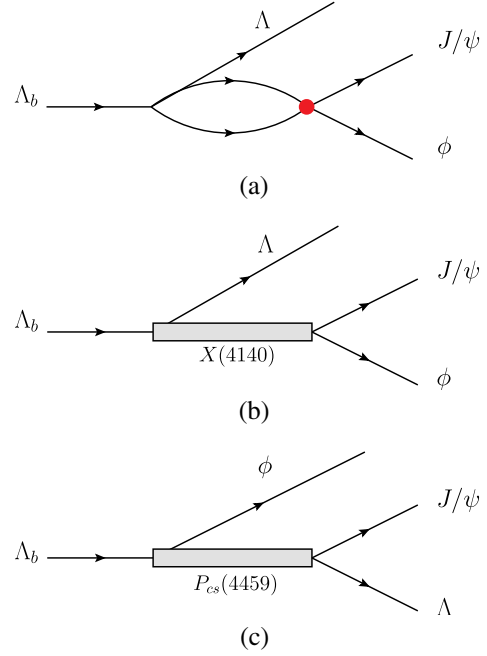


FIG. 2. Mechanism to produce the $J/\psi \Lambda \phi$ final state through $X(4160)$, $X(4140)$, and $P_{cs}(4459)$.

Ref. [36], in this work, we use the cutoff method and take $q_{\max} = 630$ MeV followed in Ref. [32],

$$G_{D_s^* \bar{D}_s^*} = i \int \frac{d^4 q}{(2\pi)^4} \frac{1}{q^2 - m_1^2 + i\epsilon} \frac{1}{(p-q)^2 - m_2^2 + i\epsilon} = \int_0^{q_{\max}} \frac{q^2 dq}{(2\pi)^2 \omega_1 \omega_2 [(P^0)^2 - (\omega_1 + \omega_2)^2 + i\epsilon]}, \quad (7)$$

where $m_{1,2}$ are the masses of D_s^* and \bar{D}_s^* , $\omega_i = \sqrt{|\vec{q}_i|^2 + m_i^2}$ are the energies of D_s^* and \bar{D}_s^* , and $P^0 = \sqrt{s}$ is the center-of-mass energy. And the transition amplitude is given by

$$t_{D_s^* \bar{D}_s^* \rightarrow J/\psi \phi} = \frac{g_{J/\psi \phi} g_{D_s^* \bar{D}_s^*}}{M_{J/\psi \phi}^2 - M_{X(4160)}^2 + iM_{X(4160)} \Gamma_{X(4160)}}, \quad (8)$$

with the couplings $g_{D_s^* \bar{D}_s^*}$ and $g_{J/\psi \phi}$ obtained in Ref. [33], the $X(4160)$ mass $M_{X(4160)} = 4156$ MeV [28]. For the $X(4160)$ width $\Gamma_{X(4160)}$, we take into account the Flatté effect for the opening of the important $D_s^* \bar{D}_s^*$ channel above the $D_s^* \bar{D}_s^*$ threshold as follows:

$$\Gamma_{X(4160)} = \Gamma_0 + \Gamma_{J/\psi \phi} + \Gamma_{D_s^* \bar{D}_s^*}, \quad (9)$$

$$\Gamma_{J/\psi \phi} = \frac{|g_{J/\psi \phi}|^2 \tilde{P}_\phi}{8\pi M_{X(4160)}^2}, \quad (10)$$

$$\Gamma_{D_s^* \bar{D}_s^*} = \frac{|g_{D_s^* \bar{D}_s^*}|^2 \tilde{P}_{D_s^*}}{8\pi M_{X(4160)}^2} \Theta(M_{J/\psi \phi} - 2m_{D_s^*}), \quad (11)$$

$$\tilde{p}_\phi = \frac{\lambda^{1/2}(M_{J/\psi\phi}^2, m_{J/\psi}^2, m_\phi^2)}{2M_{J/\psi\phi}}, \quad (12)$$

$$\tilde{p}_{D_s^*} = \frac{\lambda^{1/2}(M_{J/\psi\phi}^2, m_{D_s^*}^2, m_{D_s^*}^2)}{2M_{J/\psi\phi}}, \quad (13)$$

where Γ_0 is taken as 65.0 MeV by fitting to the LHCb data of the $B^+ \rightarrow J/\psi\phi K^+$ process [31], \tilde{p}_ϕ and $\tilde{p}_{D_s^*}$ are, respectively, the momenta of ϕ and D_s^* in the rest frame of $J/\psi\phi$. $\lambda(x, y, z) = x^2 + y^2 + z^2 - 2xy - 2xz - 2yz$ is the Källén function.

On the other hand, the $X(4140)$ state was observed in the $J/\psi\phi$ invariant mass distribution of the process $B^+ \rightarrow J/\psi\phi K^+$ [28] and could be interpreted as the $\chi_{c1}(3P)$ state [29,30]; thus, the decay $\Lambda_b \rightarrow J/\psi\phi\Lambda$ can also happen through the intermediate resonance $X(4140)$ with Λ in S wave, and the corresponding amplitude can be expressed as

$$\mathcal{M}^S = B \times \frac{M_{X(4140)}^3 \vec{\epsilon}_{J/\psi} \cdot \vec{\epsilon}_\phi}{M_{J/\psi\phi}^2 - M_{X(4140)}^2 + iM_{X(4140)}\Gamma_{X(4140)}}, \quad (14)$$

where the parameter B , with the same dimension as A , accounts for the relative weight of the contribution from the intermediate resonance $X(4140)$. We take $M_{X(4140)} = 4135$ MeV and $\Gamma_{X(4140)} = 19$ MeV [28]. Since the $\Lambda_b \rightarrow J/\psi\phi\Lambda$ process has been observed by the CMS Collaboration [8], we will show our results up to an arbitrary normalization, and our predictions can be tested while enough data sample are available in future.

As we discussed above, many studies favor the quantum numbers $J^P = 1/2^-$ for the $P_{cs}(4459)$ [21,37,38], which implies that the $P_{cs}(4459)$ couples to $J/\psi\Lambda$ in S wave, and the Λ_b weakly decays into $P_{cs}(4459)\phi$ in S wave, as depicted in Fig. 2(c). The amplitude for the contribution of $P_{cs}(4459)$ can be expressed as

$$\mathcal{M}^{P_{cs}} = C \times \frac{M_{P_{cs}}^3 \vec{\epsilon}_{J/\psi} \cdot \vec{\epsilon}_\phi}{M_{J/\psi\Lambda}^2 - M_{P_{cs}}^2 + iM_{P_{cs}}\Gamma_{P_{cs}}}, \quad (15)$$

where we take $M_{P_{cs}} = 4458.8$ MeV and $\Gamma_{P_{cs}} = 17.3$ MeV [20], and the parameter C stands for the relative weight of the contribution from $P_{cs}(4459)$.

With the amplitudes of Eqs. (6), (14), and (15), the mass distribution of the $\Lambda_b \rightarrow J/\psi\phi\Lambda$ process is given by

$$\frac{d^2\Gamma}{dM_{J/\psi\phi}^2 dM_{J/\psi\Lambda}^2} = \frac{1}{(2\pi)^3} \frac{1}{32M_{\Lambda_b}^3} \sum |\mathcal{M}|^2, \quad (16)$$

with

$$\sum |\mathcal{M}|^2 = \sum (|\mathcal{M}^S|^2 + |\mathcal{M}^P|^2) \quad (17)$$

$$= B^2(3|\tilde{\mathcal{M}}^S|^2 + 2|\vec{k}|^2|\tilde{\mathcal{M}}^P|^2), \quad (18)$$

$$\tilde{\mathcal{M}}^P = \alpha G_{D_s^* \bar{D}_s^* \Lambda} \vec{\epsilon}_{D_s^*} \cdot \vec{\epsilon}_{\bar{D}_s^*}, \quad (19)$$

$$\begin{aligned} \tilde{\mathcal{M}}^S = & \frac{M_{X(4140)}^3}{M_{J/\psi\phi}^2 - M_{X(4140)}^2 + iM_{X(4140)}\Gamma_{X(4140)}} \\ & + \frac{\beta M_{P_{cs}}^3}{M_{J/\psi\Lambda}^2 - M_{P_{cs}}^2 + iM_{P_{cs}}\Gamma_{P_{cs}}}, \end{aligned} \quad (20)$$

where $\alpha = A/B$ and $\beta = C/B$ stand for the relative weights of the $X(4160)$ and $P_{cs}(4459)$ terms with respect to the $X(4140)$ term, and we take $\alpha = \alpha_0 = 2100$ in order to give roughly equal strengths for $X(4140)$ and $X(4160)$, as done in Refs. [31,34]. It should be pointed out that there is no interference between the S wave and P wave, and the sum over the J/ψ and ϕ polarizations is

$$\sum_{\text{pol}} [(\vec{\epsilon}_{J/\psi} \times \vec{\epsilon}_\phi) \cdot \vec{k}]^2 = 2\delta^{il} k^i k^l = 2|\vec{k}|^2, \quad (21)$$

$$\sum_{\text{pol}} (\vec{\epsilon}_{J/\psi} \cdot \vec{\epsilon}_\phi)^2 = 3. \quad (22)$$

B. The $\Lambda_b \rightarrow D_s^* \bar{D}_s^* \Lambda$ process

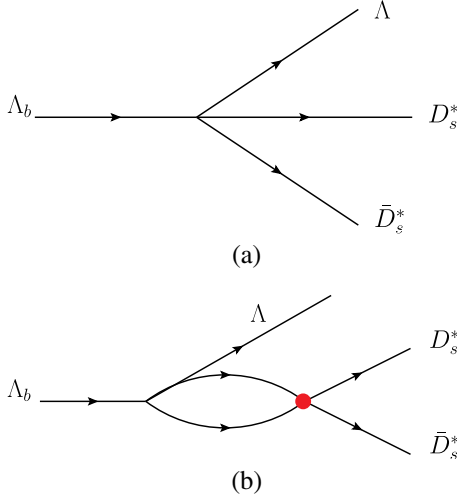
Since the width of the $X(4160)$ is 139_{-60}^{+110} MeV [28], and its mass is close to one of the $X(4140)$, the signal of the bump structure from the $X(4160)$ is usually difficult to be identified. Because the $X(4160)$ is predicted to couple strongly to the $D_s^* \bar{D}_s^*$ channel, it is expected to give rise to an enhancement structure near threshold in the $D_s^* \bar{D}_s^*$ invariant mass distribution. Thus, it is also interesting to investigate the $\Lambda_b \rightarrow D_s^* \bar{D}_s^* \Lambda$ process. The mechanism of this process can also be depicted in Figs. 1(b) and 1(c), and we will take into account the contributions from the tree level diagram of Fig. 3(a) and the $D_s^* \bar{D}_s^*$ final state interaction of Fig. 3(b). The amplitudes for both diagrams can be expressed as

$$\mathcal{M}^S = D \times k_{\text{ave}} \vec{\epsilon}_{D_s^*} \cdot \vec{\epsilon}_{\bar{D}_s^*} \quad (23)$$

for Λ in S wave and

$$\mathcal{M}^P = E(\vec{\epsilon}_{D_s^*} \times \vec{\epsilon}_{\bar{D}_s^*}) \cdot \vec{k}' (1 + G_{D_s^* \bar{D}_s^* \Lambda}) \quad (24)$$

for Λ in P wave, where $\vec{\epsilon}_{D_s^*}$ and $\vec{\epsilon}_{\bar{D}_s^*}$ are the polarization vectors of the D_s^* and \bar{D}_s^* , respectively, and \vec{k}' is the Λ momentum in the $D_s^* \bar{D}_s^*$ system. We introduce $k_{\text{ave}} = 1000$ MeV to have the parameters D and E with same dimension. The loop function is given by Eq. (7), and the transition amplitude can be expressed as


 FIG. 3. Mechanism to produce the $D_s^* \bar{D}_s^*$ final state.

$$t_{D_s^* \bar{D}_s^* \rightarrow D_s^* \bar{D}_s^*} = \frac{g_{D_s^* \bar{D}_s^*} g_{D_s^* \bar{D}_s^*}}{M_{D_s^* \bar{D}_s^*}^2 - M_{X(4160)}^2 + i M_{X(4160)} \Gamma_{X(4160)}}. \quad (25)$$

Finally, the $D_s^* \bar{D}_s^*$ invariant mass distribution of the $\Lambda_b \rightarrow D_s^* \bar{D}_s^* \Lambda$ process is given by

$$\frac{d\Gamma}{dM_{D_s^* \bar{D}_s^*}} = \frac{1}{(2\pi)^3} \frac{1}{4M_{\Lambda_b}^2} p_{\Lambda} \tilde{p}_{D_s^*} \sum |\mathcal{M}|^2, \quad (26)$$

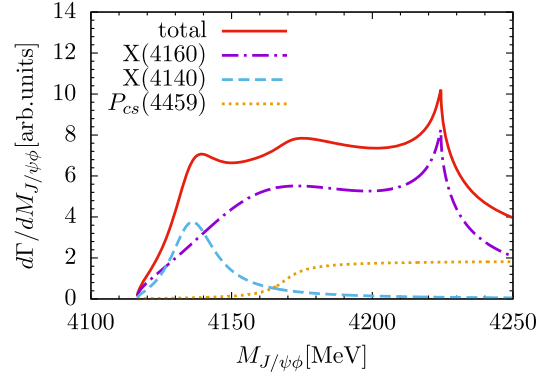
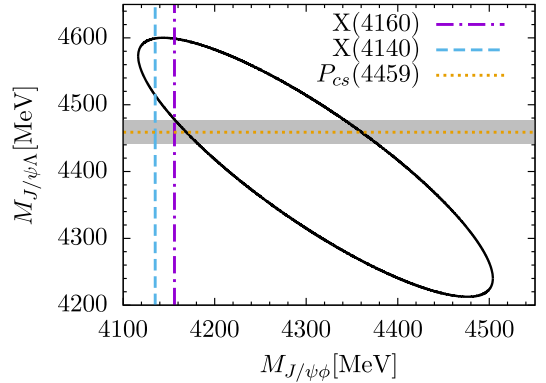
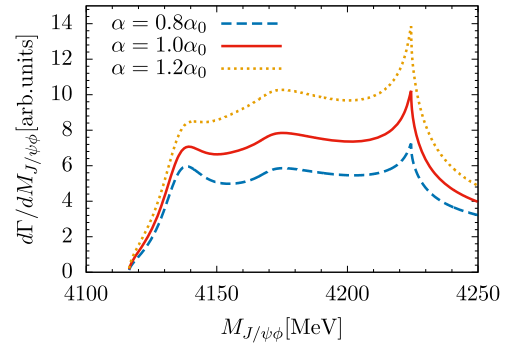
$$|\mathcal{M}|^2 = D^2 (3|k_{\text{ave}}^2| + 2|\vec{k}'|^2) |\tilde{\mathcal{M}}^P|^2, \quad (27)$$

$$\tilde{\mathcal{M}}^P = \gamma (1 + G_{D_s^* \bar{D}_s^*} t_{D_s^* \bar{D}_s^* \rightarrow D_s^* \bar{D}_s^*}),$$

with $\gamma = E/D$. p_{Λ} is the Λ momentum in the rest frame of the Λ_b , and $\tilde{p}_{D_s^*}$ is the D_s^* momentum in the rest frame of the $D_s^* \bar{D}_s^*$ system.

III. RESULTS AND DISCUSSIONS

In this section, we will present our results. With the $\beta = 1$, we show the $J/\psi\phi$ mass distribution in Fig. 4. We can find a peak around 4140 MeV, corresponding to $X(4140)$ resonance, and a bump around 4160 MeV followed by a cusp around $D_s^* \bar{D}_s^*$ threshold, which can be associated to the resonance $X(4160)$. It should be stressed that a molecular state that couples to several hadron-hadron channels may develop a strong and unexpected cusp in the invariant mass distribution in one of the weakly coupled channels at the threshold of the channels which are the main components of the state [31,32,39,40]. The intermediate $P_{cs}(4459)$ only plays an important role above the 4160 MeV, which can be easily understood according to the Dalitz plot of Fig. 5, and will shift the bump position of the $X(4160)$ to high energies. In Fig. 6, we show the $J/\psi\phi$ invariant mass distribution for different values of α , and one


 FIG. 4. The $J/\psi\phi$ invariant mass distribution of the $\Lambda_b \rightarrow J/\psi\phi\Lambda$ process. The curves labeled as “ $X(4160)$ ”, “ $X(4140)$ ”, and “ $P_{cs}(4459)$ ” show the contributions from the molecular state $X(4160)$, the intermediate resonances $X(4140)$ and $P_{cs}(4459)$, respectively. The curve labeled “total” corresponds to the total contributions of Eq. (17).

 FIG. 5. The Dalitz plot of the $\Lambda_b \rightarrow J/\psi\phi\Lambda$ process.

 FIG. 6. The $J/\psi\phi$ invariant mass distribution of the $\Lambda_b \rightarrow J/\psi\phi\Lambda$ process with different values of α ($= 0.8\alpha_0, 1.0\alpha_0, 1.2\alpha_0$).

can easily find that the bump of $X(4160)$ is clearer for the larger α .

In Fig. 7, we show the $J/\psi\Lambda$ invariant mass distribution of the $\Lambda_b \rightarrow J/\psi\phi\Lambda$ and predict a clear peak around 4460 MeV, associated to the hidden-charm pentaquark

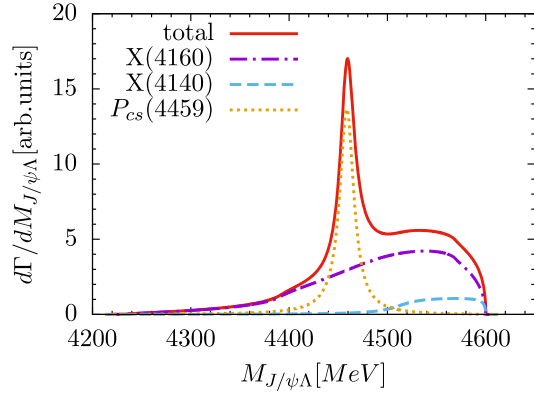


FIG. 7. The $J/\psi\Lambda$ invariant mass distribution of the $\Lambda_b \rightarrow J/\psi\phi\Lambda$ process. The explanations of the curves are the same as those of Fig. 4.

$P_{cs}(4459)$. The $X(4140)$ and $X(4160)$ resonances only have contribution in the region of $M_{J/\psi\Lambda} > 4500$ MeV and $M_{J/\psi\Lambda} > 4400$ MeV, respectively, and they do not significantly affect the peak position of the $P_{cs}(4459)$, which can be understood through the Dalitz plot of Fig. 5. We also show the $J/\psi\Lambda$ invariant mass distribution with different values of β , the relative production weight of the $P_{cs}(4459)$, in Fig. 8. It should be pointed out that we do not know the exact value of β , which should be determined by comparing with the measurements. Since $P_{cs}(4459)$ was observed in the $J/\psi\Lambda$ invariant mass spectrum of the $\Xi_b \rightarrow J/\psi\Lambda K$, it is expected that there is a signal of $P_{cs}(4459)$ in the $J/\psi\Lambda$ invariant mass distribution of $\Lambda_b \rightarrow J/\psi\Lambda\phi$. To confirm the existence of the $P_{cs}(4459)$, it is necessary to observe this state in another different process, which would strengthen its interpretation as exotic state [21,37,38], rather than possible kinematical effects.

As we mentioned above, the signal of the bump structure from $X(4160)$ is usually difficult to be identified in the $J/\psi\phi$ mass spectrum, because the width of the $X(4160)$ is

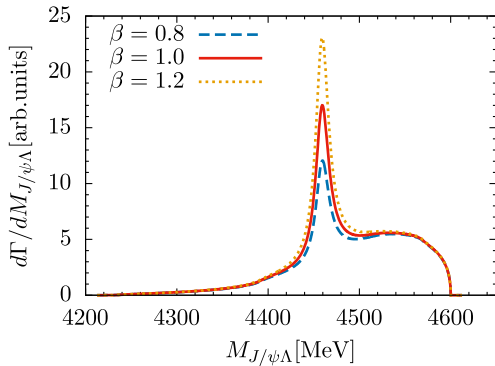


FIG. 8. The $J/\psi\Lambda$ invariant mass distribution of the $\Lambda_b \rightarrow J/\psi\phi\Lambda$ process with different values of β ($= 0.8, 1.0, 1.2$).

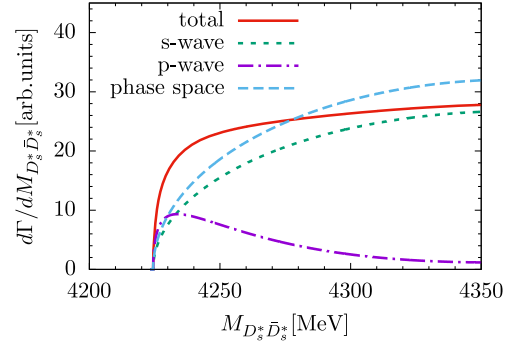


FIG. 9. The $D_s^*\bar{D}_s^*$ invariant mass distribution of the $\Lambda_b \rightarrow D_s^*\bar{D}_s^*\Lambda$ process. The curves labeled as “S wave” and “P wave” show the contributions from the S wave of Eq. (23) and the P wave of Eq. (24). The curve labeled as “total” corresponds to the total contributions of Eq. (26), and the curve labeled as “phase space” is the phase space distribution, which is normalized to the same area from threshold to 4350 MeV.

too large and its mass is close to the one of the $X(4140)$. Searching for the signal of the $X(4160)$ in other channels is also important. Although the mass of the $X(4160)$ is less than that of the $D_s^*\bar{D}_s^*$ threshold, we expect it causes an enhancement structure near the $D_s^*\bar{D}_s^*$ threshold in the $D_s^*\bar{D}_s^*$ mass spectrum, since the $X(4160)$ is predicted to couple strongly to the $D_s^*\bar{D}_s^*$ channel within the hidden gauge formalism [33]. In Fig. 9, we present the $D_s^*\bar{D}_s^*$ invariant mass distribution of the $\Lambda_b \rightarrow D_s^*\bar{D}_s^*\Lambda$ process with $\gamma = 1$. There is a significant enhancement close to the threshold with respect to the phase space distribution, which is the reflection of the $X(4160)$ and should not be misidentified with a new resonance. We also show the results for the different values of γ in Fig. 10, where one can see that the enhancement structure close to the threshold is always clear for the different values of γ . Our prediction can be tested by future measurements about the $\Lambda_b \rightarrow D_s^*\bar{D}_s^*\Lambda$ reaction.

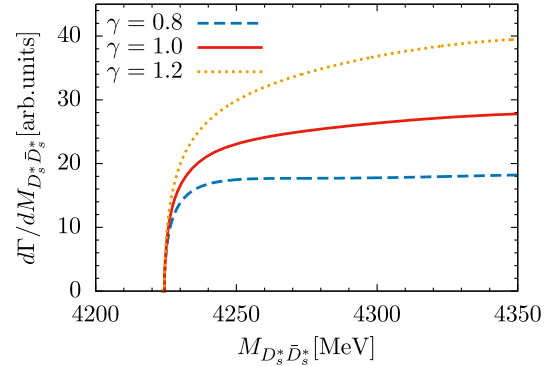


FIG. 10. The $D_s^*\bar{D}_s^*$ invariant mass distribution of the $\Lambda_b \rightarrow D_s^*\bar{D}_s^*\Lambda$ process with different values of γ .

IV. CONCLUSIONS

In this work, we have investigated the $\Lambda_b \rightarrow J/\psi \Lambda \phi$, by taking into account the $X(4140)$, $X(4160)$, and $P_{cs}(4459)$, and including the mechanisms of the W^- internal and external emissions. In the $J/\psi \phi$ mass distribution, one can find a clear peak of $X(4140)$, and a bump structure around 4160 MeV followed by a cusp structure around $D_s^* \bar{D}_s^*$ threshold, which can be associated to the $X(4160)$. We also expect that the hidden-charm pentaquark with strangeness $P_{cs}(4459)$, recently observed by the LHCb Collaboration, causes a clear peak in the $J/\psi \Lambda$ invariant mass distribution. It should be noted that it is necessary to confirm this state in another process, which would strengthen its interpretation as exotic state, rather than possible kinematical effects.

Indeed, the signal of the bump structure from the $X(4160)$ is usually difficult to be identified in the $J/\psi \phi$ mass spectrum with the low data sample, because the width of the $X(4160)$ is too large, and its mass is close to one of the $X(4140)$. Although the mass of $X(4160)$ is less than that of the $D_s^* \bar{D}_s^*$ threshold, we have predicted that there is an enhancement structure near the $D_s^* \bar{D}_s^*$ threshold in the

$D_s^* \bar{D}_s^*$ mass spectrum, since the $X(4160)$ is predicted to couple strongly to the $D_s^* \bar{D}_s^*$ channel in the hidden gauge formalism [33].

In summary, we strongly suggest further measurements of these two processes to clarify the nature of $X(4140)$ and $X(4160)$ resonances, and to confirm the existence of the $P_{cs}(4459)$.

ACKNOWLEDGMENTS

This work was partly supported by the National Natural Science Foundation of China under Grant No. 11947089. It was also supported by the Key Research Projects of Henan Higher Education Institutions under No. 20A140027, the Project of Youth Backbone Teachers of Colleges and Universities of Henan Province (2020GGJS017), the Natural Science Foundation of Henan (212300410123), the Fundamental Research Cultivation Fund for Young Teachers of Zhengzhou University (JC202041042), and the Academic Improvement Project of Zhengzhou University.

-
- [1] N. Brambilla, S. Eidelman, C. Hanhart, A. Nefediev, C. P. Shen, C. E. Thomas, A. Vairo, and C. Z. Yuan, The XYZ states: Experimental and theoretical status and perspectives, *Phys. Rep.* **873**, 1 (2020).
 - [2] H. X. Chen, W. Chen, X. Liu, and S. L. Zhu, The hidden-charm pentaquark and tetraquark states, *Phys. Rep.* **639**, 1 (2016).
 - [3] Y. R. Liu, H. X. Chen, W. Chen, X. Liu, and S. L. Zhu, Pentaquark and tetraquark states, *Prog. Part. Nucl. Phys.* **107**, 237 (2019).
 - [4] F. K. Guo, C. Hanhart, U. G. Meißner, Q. Wang, Q. Zhao, and B. S. Zou, Hadronic molecules, *Rev. Mod. Phys.* **90**, 015004 (2018).
 - [5] E. Oset, W. H. Liang, M. Bayar, J. J. Xie, L. R. Dai, M. Albaladejo, M. Nielsen, T. Sekihara, F. Navarra, L. Roca *et al.*, Weak decays of heavy hadrons into dynamically generated resonances, *Int. J. Mod. Phys. E* **25**, 1630001 (2016).
 - [6] R. Aaij *et al.* (LHCb Collaboration), Observation of $J/\psi p$ Resonances Consistent with Pentaquark States in $\Lambda_b^0 \rightarrow J/\psi K^- p$ Decays, *Phys. Rev. Lett.* **115**, 072001 (2015).
 - [7] R. Aaij *et al.* (LHCb Collaboration), Observation of a Narrow Pentaquark State, $P_c(4312)^+$, and of Two-Peak Structure of the $P_c(4450)^+$, *Phys. Rev. Lett.* **122**, 222001 (2019).
 - [8] A. M. Sirunyan *et al.* (CMS Collaboration), Observation of the $\Lambda_b^0 \rightarrow J/\psi \Lambda \phi$ decay in proton-proton collisions at $\sqrt{s} = 13$ TeV, *Phys. Lett. B* **802**, 135203 (2020).
 - [9] J. J. Wu, R. Molina, E. Oset, and B. S. Zou, Dynamically generated N^* and Λ^* resonances in the hidden charm sector around 4.3 GeV, *Phys. Rev. C* **84**, 015202 (2011).
 - [10] J. X. Lu, E. Wang, J. J. Xie, L. S. Geng, and E. Oset, The $\Lambda_b \rightarrow J/\psi K^0 \Lambda$ reaction and a hidden-charm pentaquark state with strangeness, *Phys. Rev. D* **93**, 094009 (2016).
 - [11] H. X. Chen, L. S. Geng, W. H. Liang, E. Oset, E. Wang, and J. J. Xie, Looking for a hidden-charm pentaquark state with strangeness $S = -1$ from Ξ_b^- decay into $J/\psi K^- \Lambda$, *Phys. Rev. C* **93**, 065203 (2016).
 - [12] A. Feijoo, V. K. Magas, A. Ramos, and E. Oset, A hidden-charm $S = -1$ pentaquark from the decay of Λ_b into $J/\psi, \eta \Lambda$ states, *Eur. Phys. J. C* **76**, 446 (2016).
 - [13] V. V. Anisovich, M. A. Matveev, J. Nyiri, A. V. Sarantsev, and A. N. Semenova, Nonstrange and strange pentaquarks with hidden charm, *Int. J. Mod. Phys. A* **30**, 1550190 (2015).
 - [14] Z. G. Wang, Analysis of the $\frac{1}{2}^\pm$ pentaquark states in the diquark–diquark–antiquark model with QCD sum rules, *Eur. Phys. J. C* **76**, 142 (2016).
 - [15] R. Chen, J. He, and X. Liu, Possible strange hidden-charm pentaquarks from $\Sigma_c^{(*)} \bar{D}_s^*$ and $\Xi_c^{('*)} \bar{D}^*$ interactions, *Chin. Phys. C* **41**, 103105 (2017).
 - [16] C. W. Xiao, J. Nieves, and E. Oset, Prediction of hidden charm strange molecular baryon states with heavy quark spin symmetry, *Phys. Lett. B* **799**, 135051 (2019).
 - [17] Q. Zhang, B. R. He, and J. L. Ping, Pentaquarks with the $qqs\bar{Q}Q$ configuration in the chiral quark model, [arXiv: 2006.01042](https://arxiv.org/abs/2006.01042).

- [18] C. W. Shen, H. J. Jing, F. K. Guo, and J. J. Wu, Exploring possible triangle singularities in the $\Xi_b^- \rightarrow K^- J/\psi \Lambda$ decay, *Symmetry* **12**, 1611 (2020).
- [19] R. Aaij *et al.* (LHCb Collaboration), Observation of the $\Xi_b^- \rightarrow J/\psi \Lambda K^-$ decay, *Phys. Lett. B* **772**, 265 (2017).
- [20] M. Wang (LHCb Collaboration), *Implications Workshop* (2020), <https://indico.cern.ch/event/857473/timetable/#32-exotic-hadrons-experimental>.
- [21] H. X. Chen, W. Chen, X. Liu, and X. H. Liu, Establishing the first hidden-charm pentaquark with strangeness, [arXiv:2011.01079](https://arxiv.org/abs/2011.01079).
- [22] T. Aaltonen *et al.* (CDF Collaboration), Evidence for a Narrow Near-Threshold Structure in the $J/\psi \phi$ Mass Spectrum in $B^+ \rightarrow J/\psi \phi K^+$ Decays, *Phys. Rev. Lett.* **102**, 242002 (2009).
- [23] S. Chatrchyan *et al.* (CMS Collaboration), Observation of a peaking structure in the $J/\psi \phi$ mass spectrum from $B^\pm \rightarrow J/\psi \phi K^\pm$ decays, *Phys. Lett. B* **734**, 261 (2014).
- [24] V. M. Abazov *et al.* (D0 Collaboration), Search for the $X(4140)$ state in $B^+ \rightarrow J/\psi \phi K^+$ decays with the D0 detector, *Phys. Rev. D* **89**, 012004 (2014).
- [25] V. M. Abazov *et al.* (D0 Collaboration), Inclusive Production of the $X(4140)$ State in $p\bar{p}$ Collisions at D0, *Phys. Rev. Lett.* **115**, 232001 (2015).
- [26] R. Aaij *et al.* (LHCb Collaboration), Observation of $J/\psi \phi$ Structures Consistent with Exotic States from Amplitude Analysis of $B^+ \rightarrow J/\psi \phi K^+$ Decays, *Phys. Rev. Lett.* **118**, 022003 (2017).
- [27] R. Aaij *et al.* (LHCb Collaboration), Amplitude analysis of $B^+ \rightarrow J/\psi \phi K^+$ decays, *Phys. Rev. D* **95**, 012002 (2017).
- [28] P. A. Zyla *et al.* (Particle Data Group), Review of particle physics, *Prog. Theor. Exp. Phys.* **2020**, 083C01 (2020).
- [29] W. Hao, G. Y. Wang, E. Wang, G. N. Li, and D. M. Li, Canonical interpretation of the $X(4140)$ state within the 3P_0 model, *Eur. Phys. J. C* **80**, 626 (2020).
- [30] D. Y. Chen, Where are $\chi_{cJ}(3P)$?, *Eur. Phys. J. C* **76**, 671 (2016).
- [31] E. Wang, J. J. Xie, L. S. Geng, and E. Oset, Analysis of the $B^+ \rightarrow J/\psi \phi K^+$ data at low $J/\psi \phi$ invariant masses and the $X(4140)$ and $X(4160)$ resonances, *Phys. Rev. D* **97**, 014017 (2018).
- [32] E. Wang, J. J. Xie, L. S. Geng, and E. Oset, The $X(4140)$ and $X(4160)$ resonances in the $e^+e^- \rightarrow \gamma J/\psi \phi$ reaction, *Chin. Phys. C* **43**, 113101 (2019).
- [33] R. Molina and E. Oset, The $Y(3940)$, $Z(3930)$ and the $X(4160)$ as dynamically generated resonances from the vector-vector interaction, *Phys. Rev. D* **80**, 114013 (2009).
- [34] V. Magas, À. Ramos, R. Somasundaram, and J. Tena Vidal, Exotic hadrons in the $\Lambda_b \rightarrow J/\psi \phi \Lambda$ decay, *Phys. Rev. D* **102**, 054027 (2020).
- [35] A. Martínez Torres, K. P. Khemchandani, J. M. Dias, F. S. Navarra, and M. Nielsen, Understanding close-lying exotic charmonia states within QCD sum rules, *Nucl. Phys. A* **966**, 135 (2017).
- [36] J. J. Wu and B. S. Zou, Prediction of super-heavy N^* and Λ^* resonances with hidden beauty, *Phys. Lett. B* **709**, 70 (2012).
- [37] F. Z. Peng, M. J. Yan, M. Sánchez Sánchez, and M. P. Valderrama, The $P_{cs}(4459)$ pentaquark from a combined effective field theory and phenomenological perspectives, [arXiv:2011.01915](https://arxiv.org/abs/2011.01915).
- [38] Z. G. Wang, Analysis of the $P_{cs}(4459)$ as the hidden-charm pentaquark state with QCD sum rules, [arXiv:2011.05102](https://arxiv.org/abs/2011.05102).
- [39] L. R. Dai, J. M. Dias, and E. Oset, Disclosing $D^* \bar{D}^*$ molecular states in the $B_c^- \rightarrow \pi^- J/\psi \omega$ decay, *Eur. Phys. J. C* **78**, 210 (2018).
- [40] L. R. Dai, G. Y. Wang, X. Chen, E. Wang, E. Oset, and D. M. Li, The $B^+ \rightarrow J/\psi \omega K^+$ reaction and $D^* \bar{D}^*$ molecular states, *Eur. Phys. J. A* **55**, 36 (2019).